(Received 25 December 2023, Accepted 11 July 2024, Scheduled 25 July 2024)

A Proximity-Fed Multi-Band Printed Antenna for Wireless Communication Applications

Ali J. Salim[1,*], Jabbar K. Mohammed[2], Hussam Al-Saedi[1], and Jawad K. Ali[1]

[1] *Applied Electromagnetic Research Group, Department of Communication Engineering, University of Technology, Iraq*
[2] *Department of Electrical Engineering, University of Technology, Iraq*

ABSTRACT: This paper introduces a new triple-band antenna driven indirectly by a feed line for multiple wireless applications. The structure of this antenna is based on the creation of a set of slots and slits on the ground plane mounted on a substrate with relative permittivity of 4.4 and thickness of 1.6 mm. On the other hand, a 50-ohm microstrip feed line has been fixed. It is found that the proposed antenna offers a triple-band fashion with −10 dB impedance bandwidths suitable for most recent wireless applications. The first band extends from 1.6 GHz to 2.8 GHz, which covers LTE bands (1, 2, 3, 4, 9, 10, 23, 24, 25, 33, 34, 35, 36, 37, 39 and 40), 2.4 GHz-Bluetooth, and 2.45 GHz ISM. The second band extends from 3.38 GHz to 3.6 GHz, which covers most WiMAX applications, while the third band reconciles 5.8 GHz-ITS and 2.4/5.8 GHz-WLAN. A prototype of the proposed antenna has been successfully simulated, fabricated, and measured.

1. INTRODUCTION

Designers of microstrip or printed antennas are still looking for ways to get antennas with miniaturized size and multi-band resonant or wideband behavior to suit the continuous requirements of modern mobile devices and recent wireless applications [1].

One of the broadband techniques is inducing multiple resonances (modes), which can be approached by the use of the following [2]:

- Parasitic elements.
- Slotting patches.
- An aperture, proximity coupling.

The indirect and approximated feeding antenna approach can be reached in various forms. Firstly, some of these forms fixing the feeding element on the same side of the radiating patch spaced by a gap between them, the coordinates and size of the feeding element with respect to the radiating patch play an essential role in antenna behavior (also this form of feeding is called gap-coupled) [3–8]. Secondly, depending on the coupling of the electromagnetic field, aperture coupling is another indirect form of feeding the radiating element [9–14]. The antenna structure in this form consists of at least two substrates separated by a ground plane. The upper substrate contains the radiating patch, while the bottom substrate contains the microstrip feed line. An aperture with a finite size is created in the ground plane to enhance the coupling from the microstrip feed line to the radiating patch.

Finally, other forms, consisting of a single substrate layer, making it easy to fabricate, are included. The feed line is fixed on one side of the substrate, while the radiating slot element is on the other. Emphasis will be focused on the latter method because the design of the proposed antenna in this paper will align with this method.

Many research works have been reported concerning the design of these antennas that are indirectly fed through which the resulting bandwidth(s) can be enhanced [15–32]. This type of feeding is more desirable when being needed to improve the operating bandwidth.

However, variations in the shape of slots play a main role in the behavior of the designed antennas. Besides, wider bandwidth can be obtained by exciting more operating modes at the desired frequency. This can be achieved by introducing elements of various shapes associated with the microstrip feed line as stubs.

Many researchers have adopted fractal geometry-based shapes such as Koch, Cantor, Hilbert, Sierpinski, and other fractal curves because of these shapes' enormous advantages [15–21]. Other researchers adopted Euclidean shapes such as triangles, squares, rectangles, and other polygons in the design process [22–31].

In [15], the slot of the antenna structure has been formed by using the fractal geometry of Cantor square with the second iteration. It is found that variation in the aspect ratio of slot dimensions changes the resonant band positions.

Different shapes based on Koch fractal geometry, like snowflakes and curves, have been used with different iterations to excite more resonances to produce wide-slot antennas and bandwidth enhancement [16–19].

Besides, various fractal geometries like tree fractal and Moore spacing filling have been adopted to design different slot structures. The results demonstrated a multi-band behavior

* Corresponding author: Ali Jabbar Salim (alijalim@gmail.com).

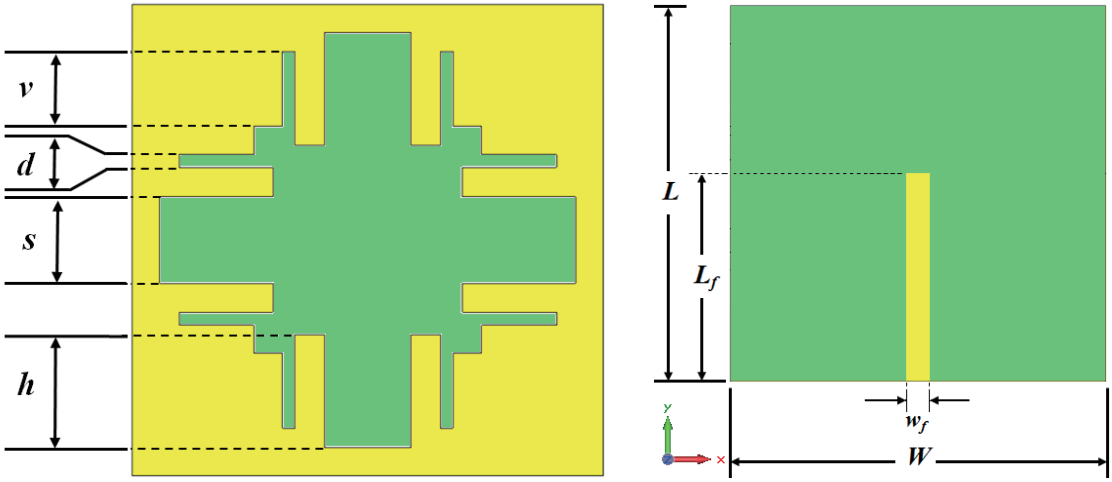

FIGURE 1. The layout of the modeled antenna. (a) Front, (b) back.

with enhanced bandwidth introduced in [20, 21]. Antennas with different slots based on H, U, and V shapes have been used to widen the bandwidth, as in [22–24]. As in [25–27], other forms, like ellipse and hexagon, have been adopted to produce different slot structures for wide bandwidth applications. Many researchers depended on conventional shapes like rectangle, triangle, square, and rhombus for multi-band and wideband antennas, as demonstrated in [28–31].

2. THE PROPOSED ANTENNA STRUCTURE

This paper introduces a new curve to create a multi-slot structure. The proposed curve is based on a set of shapes consisting of squares and rectangles with various dimensions, as shown in Fig. 1. These shapes are combined in a manner and then subtracted to create this curve to produce the multi-slot structure used in the antenna design. The method of producing the slot structure can be explained as follows. A set of slots consists of a main square slot created at the center of the ground plane and four rectangular slots; each one is aligned with each side of the main square slot. Besides, a set of four L-shaped slits has been created such that each slit has been fixed at each vertex of the main square slot, as illustrated in Fig. 1.

The multi-band behavior was achieved by creating these slots and slits that differed in shape, size, and position, as well as the arrangement of these slots and slits. Creating a slot or slit in the antenna structure makes it resonate at a new frequency (new modes), with the amount depending on the shape and size of the slot or slit. Therefore, when multiple slots and slits are created, more frequencies (modes) are generated, which results in a new multi-band antenna. In other words, creating different slots and slits in the proposed antenna generates different resonating modes. Controlling these bands can be performed by changing the dimensions and shapes of these slots and slits. The generated modes in the antenna either have frequencies close to each other or are adjacent. They will generate a wide frequency band depending on a number of these modes, or they will have frequency values far apart, generating many individual bands. In this paper, both of the above cases have occurred, represented by the lower band, and the other, middle and the higher, as will be noted in the discussion of the obtained results.

Electromagnetic numerical analysis and performance evaluation of the proposed antenna were carried out using the Microwave Studio Suite of the Computer Simulation Technology (CST) [33] and High Frequency Structure Simulator (HFSS) to validate and prove the results.

3. STEPS TO REALIZE THE PROPOSED ANTENNA

The procedure of the accomplished proposed antenna in this paper can be explained through the following five antennas using a substrate material of FR-4 with a relative permittivity of 4.6 ($\delta = 0.025$) and dimensions of 50 mm $\times$ 50 mm, as shown in Fig. 2. Each step is related to the design of an antenna until the realization of the desired antenna, and the resultant response of each antenna is shown in Fig. 3. In *antenna No. 1*, a squared-shaped slot antenna with tapered corners has been created in the center of the ground plane. It is noted that a noticeable response can be adopted. In *antenna No. 2*, rectangular slots have been created on the right and left of the main square slot in *antenna No. 1*.

A resonant bandwidth with a frequency of nearly 4.5 GHz is obtained. Then, two rectangular slots have been added above and under the main square, as shown in *antenna No. 3*. The resultant band is shifted up and centered nearly at 4.8 GHz with a low matching level. *Antenna No. 4* represents a combination of *antennas 2 and 3*; this structure starts to demonstrate a dual-band behavior at positions 2.0 GHz and 5.7 GHz. The higher band has a very low level of matching, as shown in Fig. 3, which requires an enhancement in matching to make this antenna work efficiently. An L-shaped slit is created at each vertex of the main square slot in *antenna No. 4* to produce the antenna of *antenna No. 5*, which is the final one in this search. Appropriate dimensions for these slots and slits have been chosen such that the triple-band behavior and wide bandwidth are achieved. The symmetrical geometry of the proposed antenna is maintained

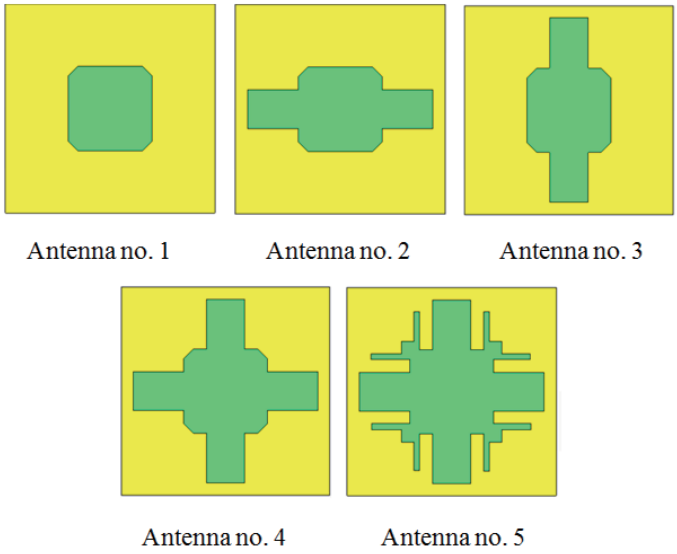

FIGURE 2. The generation process of the proposed antenna.

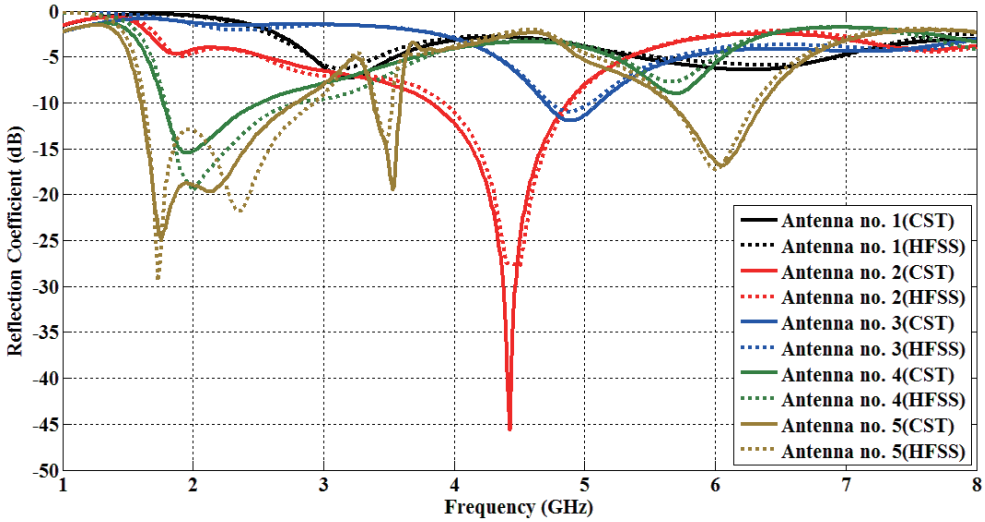

FIGURE 3. The reflection coefficient response of the five antennas.

for the purpose of keeping the same effect as the feed line on the ground plane as well as obtaining a symmetrical radiation results.

It is noted that in the fifth step, how the L-slots at each corner played a major role in supporting and strengthening the middle band, in addition to strengthening the other two bands. This is because creating the slots in this way and choosing the appropriate dimensions for them, in addition to choosing the appropriate locations in the antenna structure, leads to releasing modes operating around the specified frequency and enhancement of matching in the other two bands.

4. PERFORMANCE EVALUATION

In this section, the evaluation of antenna performance is accomplished by investigating most parameters shown in Fig. 1. It is found that some of these parameters have a significant influence on the amount of reflection coefficient in a specific band. At the same time, these parameters slightly affect the location of resonant frequency and bandwidths. In contrast, other parameters have a distinguished impact on the amount of bandwidth besides the resonant frequency.

Parameter s, as seen in Fig. 4, has a noticeable effect on the antenna performance. In the lower band, the reflection coefficient decreases as the value of s increases which in turn improves the matching level in this band. Meanwhile, antenna behavior is enhanced in the middle band with an increasing value of this parameter. In the higher band, with any increase in s value, the location of the center frequency will move up while the reflection coefficient is slightly changed.

Parameter h plays approximately the same role as parameter s in the higher and oppositely in the lower bands as noted in Fig. 5. In the middle band, it is found that this parameter can play an important role in the response shape of this antenna.

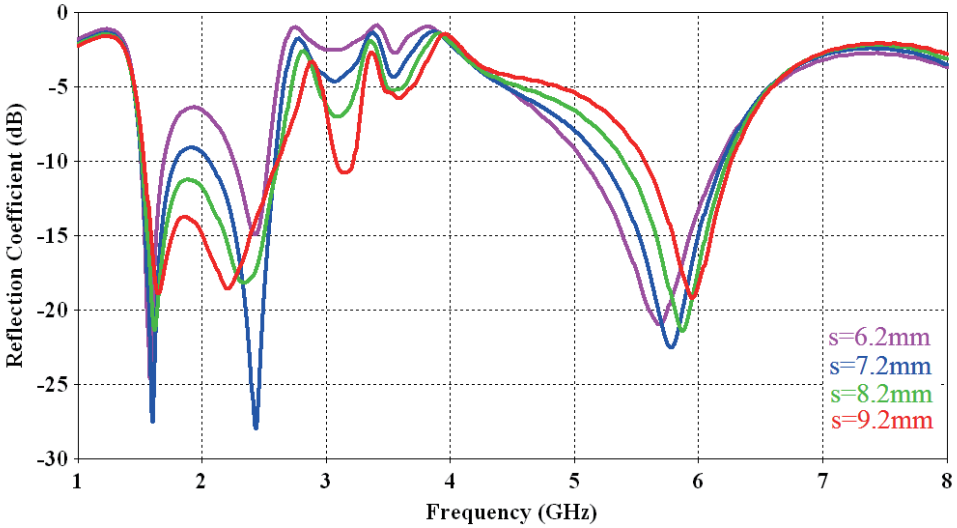

FIGURE 4. The reflection coefficient responses with s as a parameter.

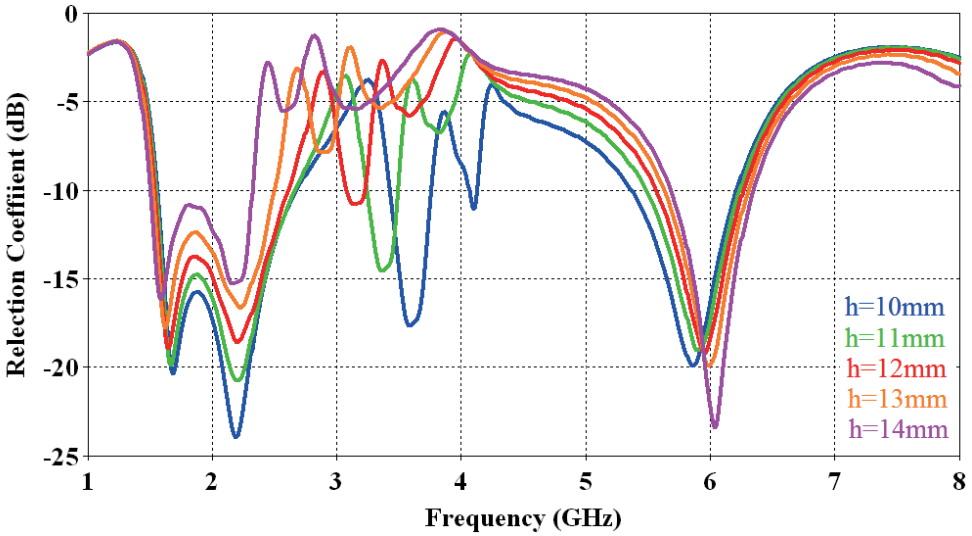

FIGURE 5. The reflection coefficient responses with h as a parameter.

The reduction of h value further enhances the matching level in this band, and at the same time, the location of the center frequency moves up.

Parameter d has the same effect on the three resultant bands regarding the matching level but at different grades, especially at the lower side of the lower band, as shown in Fig. 6. As well, this parameter affects the location of the center frequency of the middle band such that increasing the value of d leads to moving down the location of the center frequency. Considering parameter v which represents the length of the slit, this parameter plays a role concerning the locations of resonant frequencies and the level of matching, particularly the lower side of the lower band, as shown in Fig. 7. However, the significant effect of this parameter is symbolized in controlling the location of the center frequency of the middle band besides the matching level. As the value of this parameter increases, the center frequency and matching level decrease until this band vanishes. Therefore, this parameter is responsible for enhancing or suppressing the middle band by selecting an optimum value.

The length of the feeding line in the proposed antenna must be considered to demonstrate its effect on the performance of the antenna. This effect is represented by the parameter *lf*. The location of the center frequency of the higher band has been more affected by variations of feeding line length such that decreasing the length leads to moving up the location of center frequency, as shown in Fig. 8. In contrast, an increase in the length increases the matching level in the lower band, particularly in the lower side of this band. The response regarding the middle band has been relatively unaffected by the variations of the feed line length.

The purpose of investigating the influence of these parameters is to demonstrate how the appropriate value for each pa-

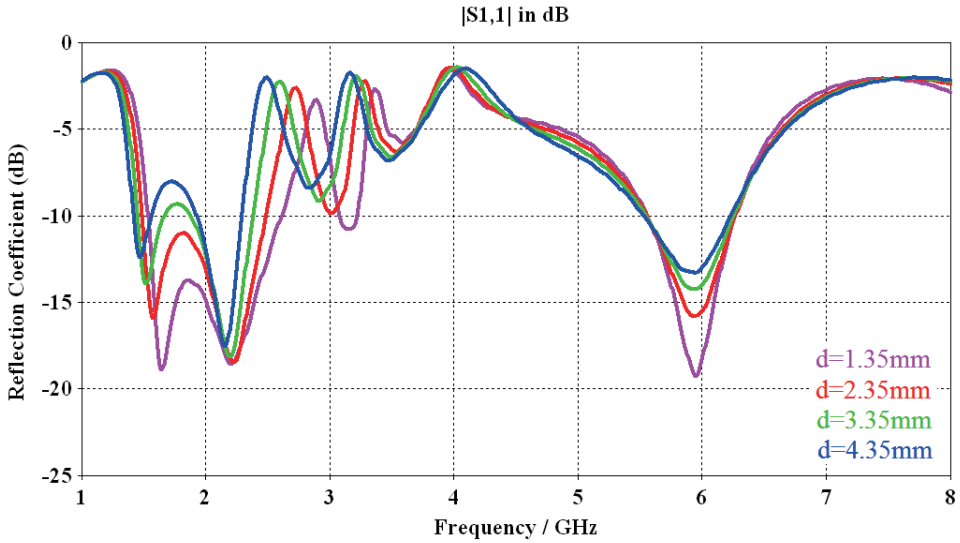

FIGURE 6. The reflection coefficient responses with d as a parameter.

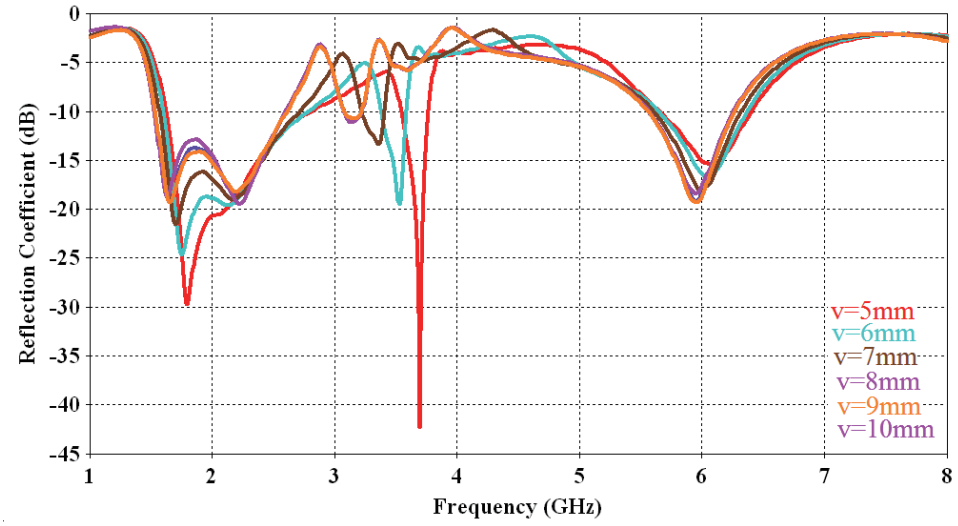

FIGURE 7. The reflection coefficient responses with v as a parameter.

rameter gives the best performance for the proposed antenna. In addition, it is noted that the most influential parameters of the middle band enhancement are h and v. In this paper, the emphasis has been focused on parameter v rather than parameter h due to fine and reasonable response. Also, some parameters are characterized by any minor change in their value, leading to a significant change in antenna response.

Finally, the appropriate values of these parameters have been listed in Table 1. Accordingly, the influence of each of the geometrical parameters on the antenna performance can be illustrated by changes in the location of center frequency and the reflection coefficient value in each of the three resultant bandwidths for the proposed antenna as summarized in Table 2 by using an indication as follows: increase (▲), robust increase (▲▲), decrease (▼), robust decrease (▼▼), and slightly changed (►◄). It was found that most of these parameters did not have evident effects on the center frequency of the lower bandwidth; somewhat, its effects have receded on determining the amount of reflection coefficient level.

TABLE 1. Parameters of the modeled antenna.

Parameter	Symbol	Value (mm)
Rectangular slot width	s	9.2
Rectangular slot height	h	12
L-shaped slit trace	d	1.35
L-shaped slit length	v	8
Feed line width	w_f	3
Feed line length	l_f	28
Substrate width	W	50
Substrate length	L	50

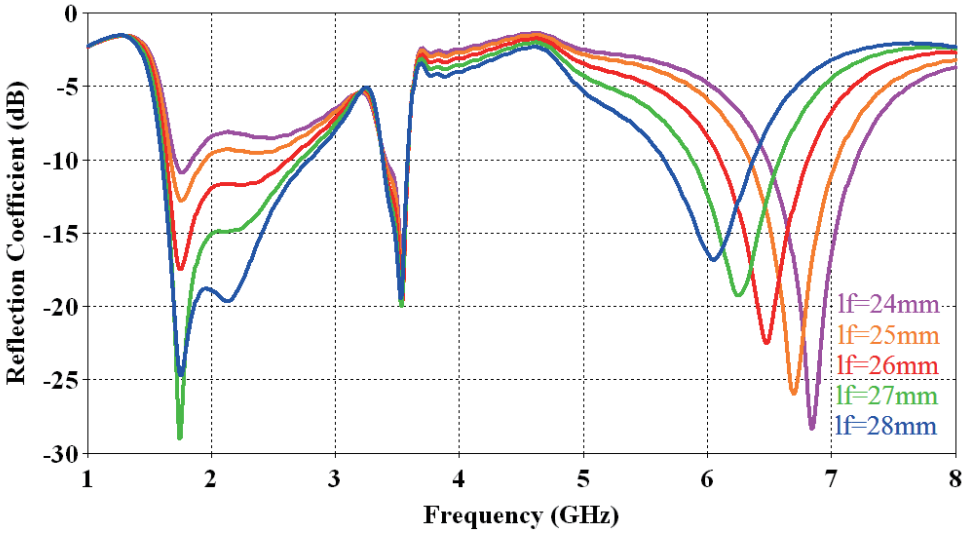

FIGURE 8. The reflection coefficient responses with *lf* as a parameter.

TABLE 2. Parameters influence of the modeled antenna on center frequencies and reflection coefficient.

Parameter	Range of variation (mm)	Step size (mm)	Frequency drift			Reflection coefficient drift		
			$(f_o)_{BW1}$	$(f_o)_{BW2}$	$(f_o)_{BW3}$	$(S_{11})_{BW1}$	$(S_{11})_{BW2}$	$(S_{11})_{BW3}$
s	*6.20–9.20*	1.0	▶◀	▶◀	▲	▼▼	▼▼	▲
h	*10.0–14.00*	1.0	▶◀	▼▼	▲	▲	▲▲	▶◀
d	*1.35–4.35*	1.0	▶◀	▼	▶◀	▲▲	▲	▲
v	*5.00–10.0*	1.0	▶◀	▼▼	▼	▲	▲	▶◀
l_f	*24.0–28.0*	1.0	▶◀	▶◀	▼▼	▼▼	▶◀	▲▲

The total length of the slot structure, which is related to the parameters in Table 1, can be determined by Equation (1):

$$Lt = 8[9 + 0.5s + h + d + v] \tag{1}$$

Meanwhile, it is noted that each of the parameters, h and v, has a significant impact on strengthening the middle bandwidth and making it operate within the required frequency besides their effects on the other bandwidths.

The geometric parameters' effects on the behavior of the middle band were different; some of these parameters had less effect. However, the most influential of these parameters were both h and v, which played a significant role in determining the location of the center frequency and the impedance matching level of this band, as noted in Table 2. Parameter *lf* has no noticeable effect. By checking the influence of different parameters on the antenna performance, it was found that the significant factor in the performance of the proposed antenna is the total length of the slot structure in terms of the guided wavelength λg:

$$\lambda_g = \frac{\lambda_\circ}{\sqrt{\varepsilon_{eff}}} \tag{2}$$

where ε_{eff} is the effective dielectric constant.

The lowest frequency *fl* that is relative to half of the L_t is expressed in Equation (3);

$$fl = \frac{c_\circ}{2L_t\sqrt{\varepsilon_{eff}}} \tag{3}$$

where $c_\circ$ is the speed of light in free space.

As said previously and noted in Table 1, the lower band was not significantly affected by the changes in geometric parameters proposed to study the behavior of the proposed antenna. This gives the impression that the total slot length derived in Equation (1) determines the frequency in the low band as in Equation (3).

It is evident that the final simulation results of the proposed antenna demonstrated a triple-band behavior with -10 dB impedance bandwidth of approximately 1.2 GHz extending from 1.6 GHz to 2.8 GHz centered at 2.2 GHz for the lower band, 0.202 GHz (202 MHz) extending from 3.38 GHz to 3.6 GHz centered at 3.49 GHz for the middle band, and 0.720 GHz (720 MHz) extending from 5.65 GHz to 6.36 GHz centered at 6 GHz for the higher band as shown in Fig. 9.

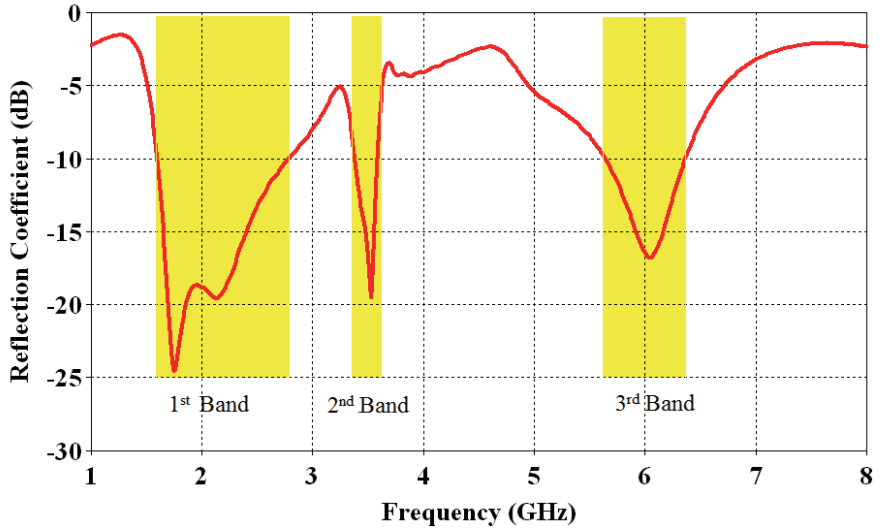

FIGURE 9. The simulated reflection coefficient response.

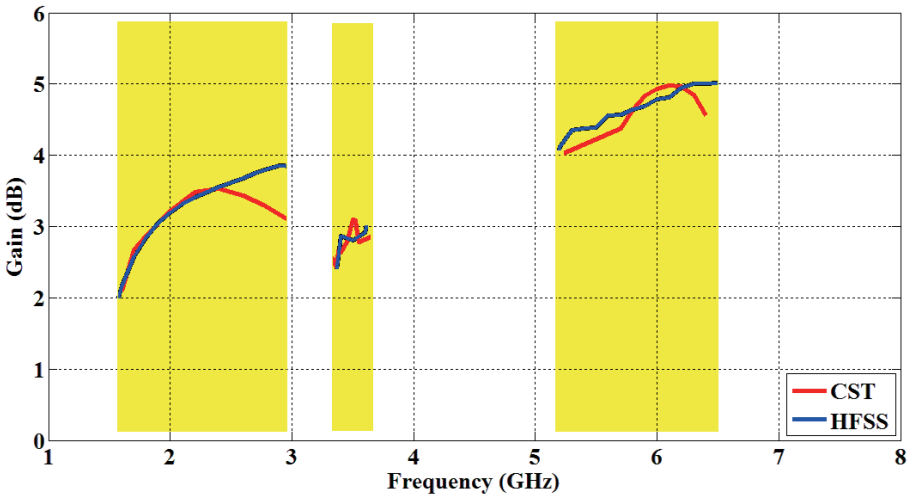

FIGURE 10. The simulated gain responses throughout: (a) lower band (b) middle band, and (c) the upper band.

5. GAIN RESULTS, RADIATION PATTERN AND SURFACE CURRENT DISTRIBUTION

The simulated gain variations versus frequency over each band are illustrated in Fig. 10. As shown from Fig. 10, using two simulators, CST and HFSS, an average gain is about 3.48 dBi (3.40 dBi) at a frequency of 2.2 GHz over the lower band and about 3.10 dBi (2.80 dBi) at a frequency of 3.5 GHz through the middle band. Over the higher band, the average gain reaches 4.64 dBi (5.35 dBi) at a frequency of 5.8 GHz, and the gain ranges at the three bands are 2.17–3.11 dBi (2.12–3.86 dBi) in the lower band, 2.51–2.86 dBi (2.55–3.10 dBi) in the middle band, and 4.13–4.58 dBi (5.14–6.54 dBi) in the higher band. It is noted that the gain variation through the middle and higher bands is nearly stable. Meanwhile, through the lower band, the gain behaves approximately in a linear change due to the wide range in this band compared to other bands.

There is a good agreement between the two simulated gains (CST and HFSS), especially in the lower band at the frequency range (1.6–2.5) GHz and acceptable agreement in the middle band except for a higher gain value in CST than that of HFSS at a frequency of 3.5 GHz. In the higher band, all gain values of HFSS are higher than those of CST, with variation less than 1.2 dBi. However, the obtained gain at three bands meets the operation needs in most of the recent wireless communication systems.

Far-field radiation pattern characteristics of the proposed antenna, for specified frequencies, have been simulated by using two simulators to verify the validity of results, as shown in Fig. 11, illustrating a polar plot of the radiation pattern in three planes; XZ ($\varphi = 0°$), XY ($\theta = 90°$), and YZ ($\varphi = 90°$). The proposed antenna demonstrates sensible radiation pattern attributes. The radiation characteristics in terms of cross-polarization were not addressed because the proposed

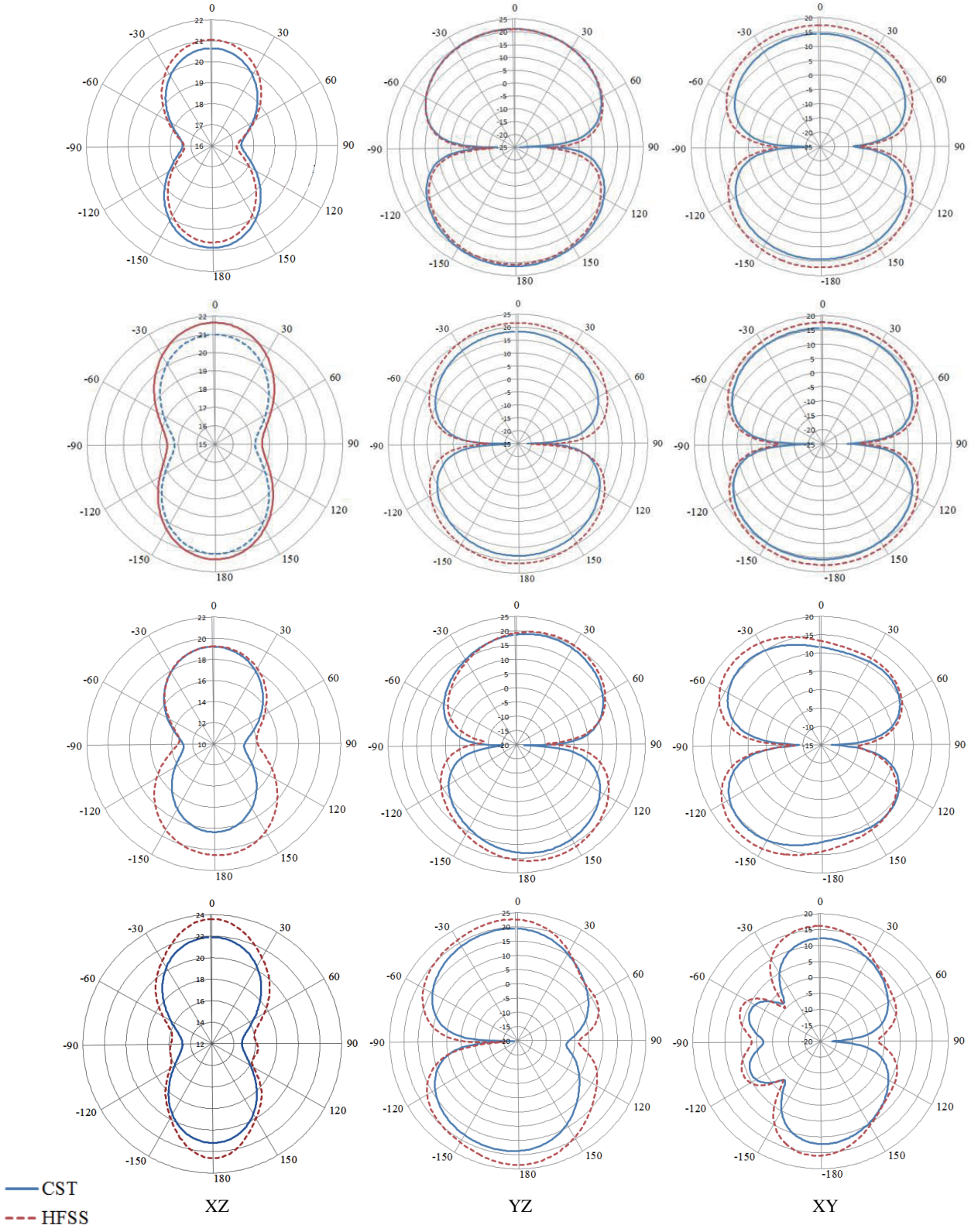

FIGURE 11. The simulated far-field radiation patterns at (a) 1.8 GHz, (b) 2.4 GHz, (c) 3.5 GHz, and (d) 5.8 GHz.

antenna did not show a circular polarization characteristic, as no technique was used to make it circularly polarized. It is necessary to discuss the surface current distribution over the resultant radiating patch; the proposed antenna especially demonstrated a multi-band behavior. At frequency 1.8 GHz, a relatively high amount of current is concentrated around the middle portion of the lower, right, and left sides of the radiating patch beside the

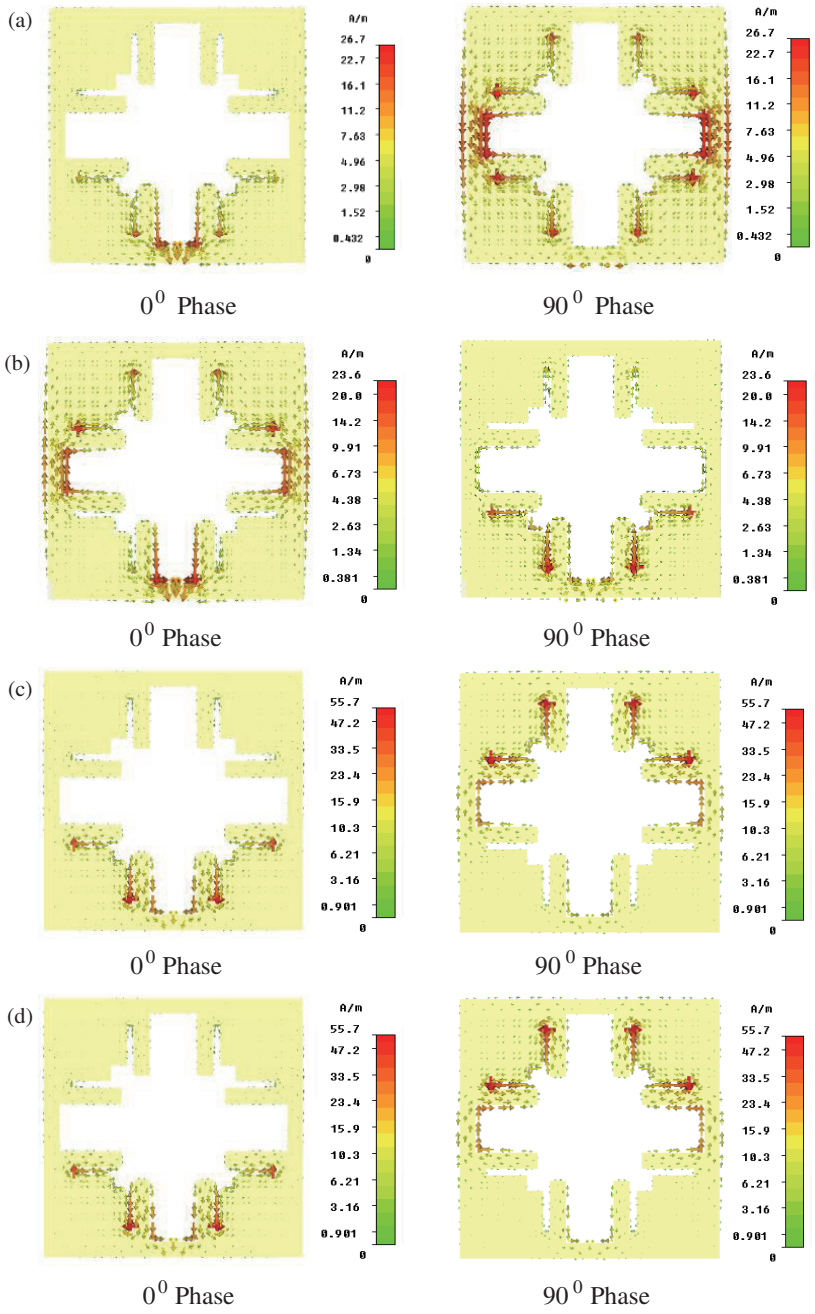

FIGURE 12. The simulated surface current distributions of the proposed antenna at (a) 1.8 GHz, (b) 2.4 GHz, (c) 3.5, and (d) 5.8 GHz.

slits on these sides, with a weak current in the middle part of the above side, as shown in Fig. 12(a).

In Fig. 12(b), which represents the surface current distribution at a frequency of 2.4 GHz, the same distribution is noted as in the case of 1.8 GHz. It is observed that the surface current is equally distributed around all sides of the radiating patch at a frequency of 3.5 GHz, as shown in Fig. 12(c).

At the frequency of 5.8 GHz, a high surface current concentrates at the middle portion of the lower side and also around the adjacent slits, as shown in Fig. 12(d), while the amount of current gradually decreases at the left and right sides up to the upper side, and the value of the current reaches the lowest level especially in the upper right and left corners. According to the above, it is noted that as the frequency increases, the current distribution begins to recede gradually, that is, it is concentrated in a specific portion only, and it is clear from comparing the current distribution at frequency 1.8 GHz with that at frequency 5.8 GHz. This is related to the electrical length resulting from the slot created in this proposed antenna, which is achieved by Equations (1) and (3), by which the total length of the slot associated with the lowest resonant frequency is calculated.

Concerning the effect of the current distribution on the radiation characteristics, due to the slots created in the proposed antenna, as we said, these slots will release many modes with frequencies that depend on the shape and dimensions of these slots. These slots have changed the distribution of the spread

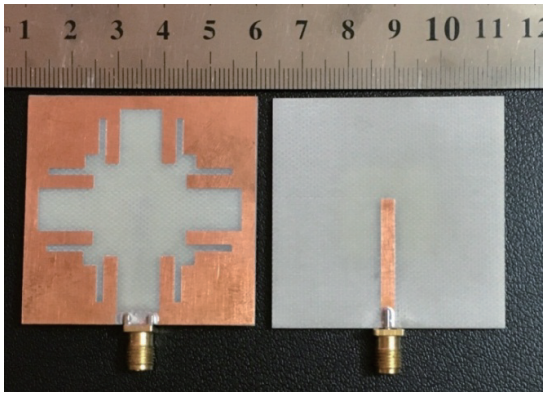

FIGURE 13. Photo of the fabricated prototype.

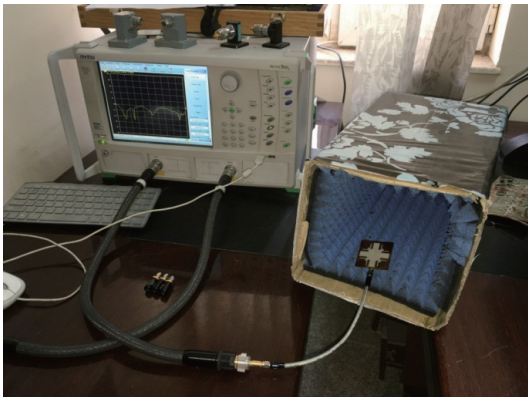

FIGURE 14. Photo of the fabricated prototype measurements.

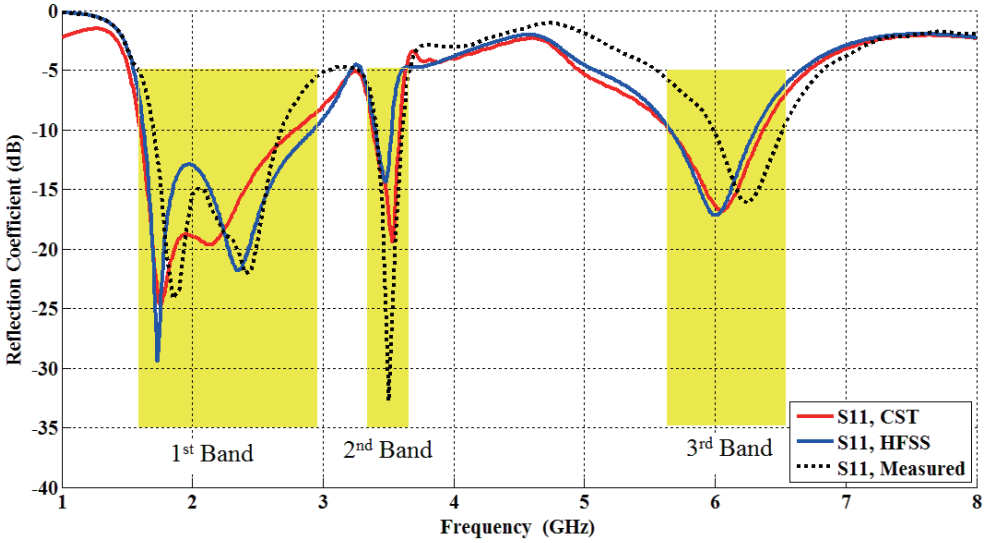

FIGURE 15. The measured and simulated reflection coefficient.

TABLE 3. Comparison of the simulated and measured results of the three bands.

	1^{st} Band			2^{nd} Band			3^{rd} Band		
	f_o (GHz)	f_L (GHz)	f_H (GHz)	f_o (GHz)	f_L (GHz)	f_H (GHz)	f_o (GHz)	f_L (GHz)	f_H (GHz)
CST	2.20	1.50	2.80	3.49	3.38	3.60	6.00	5.65	6.36
HFSS	2.26	1.61	2.92	3.46	3.39	3.54	5.97	5.65	6.30
Measured	2.17	1.65	2.70	3.50	3.40	3.60	6.25	6.00	6.50

surface current over the antenna, as there will be a pattern of specific distribution at each resonant mode. Therefore, changes in the distribution of surface currents will lead to determining the antenna's radiation pattern at each particular frequency, as evident in Figs. 11 and 12.

6. FABRICATION AND MEASUREMENTS

A photograph of the proposed antenna prototype is shown in Fig. 13. The measurement procedure has been accomplished by Anritsu MS4642A vector network analyzer, as shown in Fig. 14. The simulated and measured reflection coefficients of the proposed antenna are shown in Fig. 15. The measured bandwidths extend from 1.65 GHz to 2.7 GHz for the lower band, 3.4 GHz to 3.6 GHz for the middle band, and 6 GHz to 6.5 GHz for the higher band. By observing the simulation and measurement results, it is seen that there is a slight divergence between the results particularly in the lower and middle bands. Also, it is noted that a relatively high impedance matching is achieved at the middle band. This divergence occurred due to the soldering effect of the SMA connector, the losses from the connecting cables, and the fabrication processes involving the operations of

TABLE 4. A comparison between the cited works and the proposed one.

Ref.	Substrate thickness (mm)	Relative permittivity (ε_r)	Antenna configuration	Bandwidth frequency range, resonant frequency (GHz)	Gain (dBi)	Antenna size (mm^2)
[15]	1.6	4.4	A cantor square fractal-based slot antenna	(2.350–3.610), 2.450 (5.150–6.250), 5.800	2.86, 3.77	50×50
[16]	1.5	4.1	A Koch fractal-shaped slot antenna	(2.710–3.820), 2.980 (3.820–4.700), 4.260	5.1, 4.22	70×70
[19]	1.524	4.5	A Koch snow flack fractal-based annular slot antenna	(2.240–2.930), 2.500 (4.480–5.540), 5.200	3, 5.3	40×40
[21]	1.6	4.4	A Moore pre-fractal slot antenna	(2.350–2.520), 2.407 (3.000–3.350), 3.122 (4.000–4.400), 4.029	3.13, 3.32, 3.82	70×70
[23]	0.6	4.43	An opened U-shaped slot antenna	(0.690–0.750), 0.690 (1.700–4.200), 2.400	0.6, 2.1	65×120
[24]	0.7	4.7	An H-shaped slot antenna	(1.555–1.577), 1.575 (2.395–2.695), 2.500 (4.975–5.935), 5.800	0.26, 3.5, 3.7	60×60
[27]	1.6	4.4	A multi-polygonal-shaped slot antenna	(1.827–5.900), 3.875	4.3	72×72
[28]	1.6	4.4	A rectangular slot with a small trapezoidal slot antenna	(1.850–5.780), 3.800	4.4	92×120
[30]	1.6	4.4	A modified rhombus slot antenna	(2.210–7.420), 4.950	1.7–5.8	37.4×54
This work	1.6	4.4	A multi-slots and slits-based antenna	(1.600–2.800), 2.200 (3.380–3.600), 3.490 (5.550–6.360), 6.000	3.48, 3.10, 4.93	50×50

cutting, scraping, and drilling, which often significantly affect the measured results, particularly at high frequencies. The results of both simulation and measurements are summarized in Table 3.

It can be noted from Table 3 that the simulated lower bands using CST and HFSS are 2.2 GHz (1.5–2.8 GHz) and 2.26 GHz (1.61–2.92 GHz), respectively, while the measured lower band is 2.17 GHz (1.65–2.7 GHz). The simulated middle band is 3.49 GHz (3.38–3.6 GHz) in CST and 3.46 GHz (3.39–3.54 GHz) in HFSS, and the measured band is 3.5 GHz (3.4–3.6 GHz). Finally, the simulated higher bands 6 GHz (5.65–6.36 GHz) and 5.97 GHz (5.65–6.3 GHz) while the measured is 6.25 GHz (6–6.5 GHz).

To demonstrate the most important features shown by the proposed antenna, a comparison with the cited works is presented in Table 4. In addition to the simplicity of the profile that characterized this antenna, it showed three separated bandwidths, and one is very wide, and the gain was at rates close to or more than some of those found in the cited works. Finally, this antenna is smaller than most of the comparable antennas and the same size as some of them.

7. CONCLUSIONS

A multi-slots-based printed antenna has been designed in this paper as a candidate for 4G LTE and WLAN wireless applications. It has been found that etching slits with specific dimensions in the radiating structure led to releasing and enhancing a resonating band besides the other bands. The performance evaluation of the proposed antenna is accomplished by carrying out a parametric study to determine which antenna elements have the most significant effect on antenna behavior. The proposed antenna demonstrated a triple bands behavior with resonating frequencies centered at 2.2 GHz, 3.5 GHz, and 6 GHz, respectively. The first band is wide and tends to be 1.2 GHz, covering more than 16 bands of LTE systems, 2.4 GHz Bluetooth, and 2.45 GHz ISM. The second band extends from 3.38 GHz to 3.6 GHz, which covers most WiMax applications, while the third band reconciles 5.8 GHz-ITS and 2.4/5.8 GHz-WLAN. Moreover, the presented antenna offers high gain and sensible radiation pattern attributes.

REFERENCES

[1] Wong, K.-L., *Compact and Broadband Microstrip Antennas*, John Wiley & Sons, 2004.

[2] Chen, Z. N. and M. Y. W. Chia, *Broadband Planar Antennas: Design and Applications*, John Wiley & Sons, 2006.

[3] Solanki, M. R., K. J. Vinoy, *et al.*, "Broadband designs of a triangular microstrip antenna with a capacitive feed," *Journal of Microwaves, Optoelectronics and Electromagnetic Applications*, Vol. 7, No. 1, 44–53, Jun. 2008.

[4] Rathod, S. M., R. N. Awale, K. P. Ray, and A. D. Chaudhari, "A compact gap coupled half-hexagonal microstrip antenna with improved bandwidth," in *2017 IEEE Applied Electromagnetics Conference (AEMC)*, 1–2, Aurangabad, India, 2017.

[5] Rathod, S. M., R. N. Awale, K. P. Ray, and A. D. Chaudhari, "Broadband gap-coupled half-hexagonal microstrip antenna fed by microstrip-line resonator," *International Journal of RF and Microwave Computer-Aided Engineering*, Vol. 28, No. 6, e21273, 2018.

[6] Singh, D. K., B. K. Kanaujia, S. Dwari, G. P. Pandey, and S. Kumar, "Reconfigurable circularly polarized capacitive coupled microstrip antenna," *International Journal of Microwave and Wireless Technologies*, Vol. 9, No. 4, 843–850, 2017.

[7] Ray, K. P., V. Sevani, and S. Kakatkar, "Compact broadband gap-coupled rectangular microstrip antennas," *Microwave and Optical Technology Letters*, Vol. 48, No. 12, 2384–2389, 2006.

[8] Deshmukh, A. A. and K. P. Ray, "Broadband proximity-fed modified rectangular microstrip antennas," *IEEE Antennas and Propagation Magazine*, Vol. 53, No. 5, 41–56, Oct. 2011.

[9] Pham, N., J.-Y. Chung, and B. Lee, "A proximity-fed antenna for dual-band GPS receiver," *Progress In Electromagnetics Research C*, Vol. 61, 1–8, 2016.

[10] Lai, H. W., K. M. Mak, and K. F. Chan, "Novel aperture-coupled microstrip-line feed for circularly polarized patch antenna," *Progress In Electromagnetics Research*, Vol. 144, 1–9, 2014.

[11] Abdipour, M., S. K. Alishahi, and K. Noormohammadi, "Broadband multi-layer antenna with improved design for the applications of perfect impedance matching," *International Journal of Microwave and Wireless Technologies*, Vol. 7, No. 6, 747–752, 2014.

[12] Singh, A. and S. Singh, "Miniaturized wideband aperture coupled microstrip patch antenna by using inverted U-slot," *International Journal of Antennas and Propagation*, Vol. 2014, No. 1, 306942, 2014.

[13] Kaur, A., "Semi spiral G-shaped dual wideband microstrip antenna with aperture feeding for WLAN/WiMAX/U-NII band applications," *International Journal of Microwave and Wireless Technologies*, Vol. 8, No. 6, 931–941, 2016.

[14] Chai, W., X. Zhang, and J. Liu, "Broadband microstrip patch antenna fed by a novel coupling device," *PIERS Online*, Vol. 3, No. 7, 1064–1066, 2007.

[15] Ali, J., S. Abdulkareem, A. Hammoodi, A. Salim, M. Yassen, M. Hussan, and H. Al-Rizzo, "Cantor fractal-based printed slot antenna for dual-band wireless applications," *International Journal of Microwave and Wireless Technologies*, Vol. 8, No. 2, 263–270, 2014.

[16] Chen, W.-L., G.-M. Wang, and C.-X. Zhang, "Bandwidth enhancement of a microstrip-line-fed printed wide-slot antenna with a fractal-shaped slot," *IEEE Transactions on Antennas and Propagation*, Vol. 57, No. 7, 2176–2179, Jul. 2009.

[17] Reddy, V. V., "Broadband Koch fractal boundary printed slot antenna for ISM band applications," *Advanced Electromagnetics*, Vol. 7, No. 5, 31–36, Sep. 2018.

[18] Ali, J. K., M. T. Yassen, M. R. Hussan, and A. J. Salim, "A printed fractal based slot antenna for multi-band wireless communication applications," in *Proceedings of Progress In Electromagnetics Research Symposium, Moscow, Russia*, 19–23, Aug. 2012.

[19] Yassen, M. T., M. R. Hussan, H. A. Hammas, H. Al-Saedi, and J. K. Ali, "A dual-band printed antenna design based on annular Koch snowflake slot structure," *Wireless Personal Communications*, Vol. 104, No. 2, 649–662, 2019.

[20] Parvathy, A. R. and M. Thomaskutty, "A printed tree fractal based cross slot antenna for 2.45 GHz," *Procedia Computer Science*, Vol. 115, 80–86, 2017.

[21] Ali, J. K., "A new multiband slot antenna based on Moore spacing-filling curve geometry," in *Proceedings of IEEE Loughborough Antennas & Propagation Conference*, 449–452, Loughborough, UK, Nov. 2009.

[22] Varma, R. and J. Ghosh, "Multi-band proximity coupled microstrip antenna for wireless applications," *Microwave and Optical Technology Letters*, Vol. 60, No. 2, 424–428, 2018.

[23] Hsu, C.-K. and S.-J. Chung, "Compact antenna with U-shaped open-end slot structure for multi-band handset applications," *IEEE Transactions on Antennas and Propagation*, Vol. 62, No. 2, 929–932, Feb. 2014.

[24] Chang, T.-H. and J.-F. Kiang, "Compact multi-band H-shaped slot antenna," *IEEE Transactions on Antennas and Propagation*, Vol. 61, No. 8, 4345–4349, Aug. 2013.

[25] Kumar, M. and V. Nath, "Microstrip-line-fed elliptical wide-slot antenna with similar parasitic patch for multiband applications," *IET Microwaves, Antennas & Propagation*, Vol. 12, No. 14, 2172–2178, 2018.

[26] Kumar, B., B. K. Shukla, A. Somkuwar, and O. P. Meena, "Analysis of hexagonal wide slot antenna with parasitic element for wireless application," *Progress In Electromagnetics Research C*, Vol. 94, 145–159, 2019.

[27] Eskandari, H. and M. N. Azarmanesh, "Bandwidth enhancement of a printed wide-slot antenna with small slots," *AEU — International Journal of Electronics and Communications*, Vol. 63, No. 10, 896–900, 2009.

[28] Chen, W., "A novel broadband design of a printed rectangular slot antenna for wireless applications," *Microwave Journal*,

Vol. 49, No. 1, 122–125, Jan. 2006.

[29] Chen, W.-S. and F.-M. Hsieh, "A broadband design for a printed isosceles triangular slot antenna for wireless communications," *Microwave Journal*, Vol. 48, No. 7, 98–112, Jul. 2005.

[30] Pan, C.-Y., J.-Y. Jan, and L.-C. Wang, "Compact and broadband microstrip-line-fed modified rhombus slot antenna," *Radioengineering*, Vol. 22, No. 3, 694–699, Sep. 2013.

[31] Jan, J.-Y. and L.-C. Wang, "Printed wideband rhombus slot antenna with a pair of parasitic strips for multiband applications," *IEEE Transactions on Antennas and Propagation*, Vol. 57, No. 4, 1267–1270, 2009.

[32] CST, [Online], Available: www.CST.com.